

Data-driven Attention and Data-independent DCT based Global Context Modeling for Text-independent Speaker Recognition

Wei Xia, and John H. L. Hansen, *Fellow, IEEE*

Abstract—Learning an effective speaker representation is crucial for achieving reliable performance in speaker verification tasks. Speech signals are high-dimensional, long, and variable-length sequences that entail a complex hierarchical structure. Signals may contain diverse information at each time-frequency (TF) location. For example, it may be more beneficial to focus on high-energy parts for phoneme classes such as fricatives. The standard convolutional layer that operates on neighboring local regions cannot capture the complex TF global context information. In this study, a general global time-frequency context modeling framework is proposed to leverage the context information specifically for speaker representation modeling. First, a data-driven attention-based context model is introduced to capture the long-range and non-local relationship across different time-frequency locations. Second, a data-independent 2D-DCT based context model is proposed to improve model interpretability. A multi-DCT attention mechanism is presented to improve modeling power with alternate DCT base forms. Finally, the global context information is used to recalibrate salient time-frequency locations by computing the similarity between the global context and local features. The proposed lightweight blocks can be easily incorporated into a speaker model with little additional computational costs and effectively improves the speaker verification performance compared to the standard ResNet model and Squeeze&Excitation block by a large margin. Detailed ablation studies are also performed to analyze various factors that may impact performance of the proposed individual modules. Results from experiments show that the proposed global context modeling framework can efficiently improve the learned speaker representations by achieving channel-wise and time-frequency feature recalibration.

Index Terms—Speaker recognition, speaker embedding, attention, global context modeling, DCT transformation.

I. INTRODUCTION

AUTOMATIC Speaker Verification (ASV) involves determining a person’s identity from an input audio stream. ASV provides a natural and efficient way for biometric identity authentication. The ability to perform speaker verification is helpful in retrieving target individuals in many practical applications. Speaker recognition can be used for audio surveillance [1], computer access control, and voice authentication for telephony scenarios [2], [3]. It is also helpful for targeted

speech recognition, diarization, and separation systems if we have good speaker embeddings [4], [5], [6]. When multi-speakers in a meeting, multi-talker speaker tracking [7] is beneficial for analyzing each person’s opinion, emotion, and engagement. Smart home devices including Google Home, Amazon Alexa, and Apple Homepod could also benefit from ASV for personalized voice applications [8], [9].

Speaker verification (SV) can be categorized into two scenarios: Text-dependent speaker verification (TD-SV) and text-independent speaker verification (TI-SV). TD-SV requires the speaker to produce the same text content phrases during enrollment and test, while TI-SV verifies the speaker identity without any constraint on the speech content. Compared to TD-SV, TI-SV is more convenient because the user can speak freely to the system. However, it may require longer training and test utterances to achieve effective performance. TD-SV can also be combined with keyword spotting system (KWS) within digital assistant to enable a keyword voice authenticated wake-up service for secure voice interactions. Recent advancements in TD-SV and TI-SV have been reported using deep learning [10], [11], [12], [13] for speaker discriminative or phonetic discriminative network training. In these studies, intermediate frame-level features such as d-vectors [14], bottleneck activations or phonetic alignments are extracted to formulate utterance-level speaker representations.

Learning an effective speaker representation is crucial in speaker verification tasks. The paradigm has shifted from GMM-UBM and factor analysis based methods includes i-vector [15], [16] with a probabilistic linear discriminant (PLDA) back-end [17], [18] towards deep neural network based models. Neural network architectures such as ResNet and Time-Delay Neural Network [19], [20], [21], [22] have been explored to improve the speaker embedding extraction. Margin based softmax loss functions such as Angular Softmax [23], Additive Margin Softmax [24], Additive Angular Margin [25], Adaptive Margin [26], and Triplet loss [13], have been shown to be effective in learning discriminative speaker embeddings. Several new temporal pooling methods including attentive pooling [27], [28], Spatial Pyramid Pooling [29], and LDE [30] are able to aggregate variable length input features to a fixed-length utterance level representation. Various noise and language robust speaker recognition models [31], [11], [32], [33], training paradigms [34], [35], and domain adaptation [36], [37] methods have been proposed and significantly improve speaker verification system performance.

One basic building block for most SV models is the convo-

lutional layer, which learns filters to capture local patterns. However, the filter that only operates on the neighboring local context cannot capture long-range, non-local global information. Also, time-frequency (TF) and channel information at salient regions may not be well emphasized through a standard convolution layer. Attention mechanism is one way to improve this part. Many recent studies [38], [39], [40], [41], [42] attempt to alleviate these issues by improving the encoding of TF and channel information. One promising approach to accomplish this is the ‘‘Squeeze & Excitation’’ (SE) block [38], [43], which explicitly models the interdependencies between channels of the feature map. This SE block factors out the time-frequency dependency by average pooling to learn a channel specific descriptor, which is used to rescale the input feature map to highlight only salient channels. CBAM [44], [45] uses both global average pooling and global max pooling to obtain better performance. DAN [46] uses two types of attention modules in addition to a dilated FCN, which models the semantic interdependencies in spatial and channel dimensions, respectively. AACConv [39] uses two-dimensional relative self-attention to augment the convolution operator. Deformable network [47] designs deformable convolution to enhance the spatial modeling ability. Coordinate Attention [48] proposes a novel attention mechanism by embedding the positional information into channel attention. Non-local network [49] computes the response at a position as a weighted sum of the features at all positions to capture long-range dependencies. ECA-Net [50] uses cross-channel interaction can preserve performance while significantly decreasing model complexity. SkNet and ResNeSt [51], [52] introduce a split attention strategy with multiple branches along with different kernel sizes. The information in these branches is fused to obtain a richer representation. Many other tasks [53] also use an attention mechanism to perform context modeling for better representations. For example, ContextNet [54] and Dual-mode ASR [55] that propose a novel CNN-RNN-transducer architecture with global context information for speech recognition, Cp-GAN for speech enhancement [56], and context aware attention in speech emotion detection [57].

These channel attention approaches usually use a vector to represent the entire time-frequency information across channels. How to efficiently encode the feature map with a vector so as to preserve the collective information as much as possible is a key step in this phase of the modeling. Global Average Pooling (GAP) is the most common choice to encode the time-frequency information at a very small computational cost. However, GAP may cause inferior results in some cases and may not capture the comprehensive context information across distinct time and frequency locations. SOCA [58] proposes a second-order channel attention module to adaptively rescale the channel-wise features by using second-order feature statistics for more discriminative representations.

In this study, we propose a global time-frequency context modeling framework for speaker recognition. Speech signals contain various forms of information at each time-frequency location. For example, we may pay more attention to high energy parts in the spectrogram for some consonants such as fricatives. Our proposed approach attempts to better capture

long-range time-frequency dependencies and channel variances. First, we apply a data-driven, learnable attentive time-frequency context embedding to efficiently model the global speech contextual information. Second, we propose a data-independent 2D-DCT method to embed the time-frequency information using meaningful signal bases. With carefully designed components, the Global Time-Frequency Context (GTFC) vector is used to perform channel wise feature recalibration, and then used as an intermediate representation to enhance the local time-frequency vector bins. The attention based global context model aims to achieve a better combination of the Non-local block [49] and SE block [38], as well as using a meaningful signal processing explanation to adaptively recalibrate the learned feature map and provides time-frequency attention to specific regions.

Two-dimensional Discrete Cosine Transform (2D-DCT) is a common approach in the signal processing field. It is widely used for audio and image compression [59]. For example, Wu et al. [60] formulated a DCT based deep network for video action recognition that used a separate network for i-frames and p-frames. Ghosh et al. [61] used DCT as part of their network’s first layer and showed that it speeded up convergence for training. Ulicny et al. [62] created separate filters for each DCT basis function. DCT has been shown to be an efficient tool for frequency domain learning [63], [64] for image classification.

Here, a 2D-DCT based context model is proposed to improve the model’s interpretability and effectiveness. We show that GAP is actually a special case of attention, and 2D-DCT based context models (lowest frequency basis). When GAP is used to embed the time-frequency information into a scalar, it is possible to lose some rich audio information. Other frequency components may be a better representation of the audio signal content. With the pre-computed 2D-DCT weights, we design a multi-DCT attention framework to leverage more frequency components for global context modeling. Experimental results show that with the proposed global context modeling framework, the Equal Error Rate (EER) and the minimum Detection Cost Function (DCF) are reduced significantly.

The main contributions of this work are summarized as follows.

- A generalized global context modeling (GCT) framework is introduced by emphasizing important channel and time-frequency regions of speaker representations.
- A query-independent attention based global context model (Att-GCT) is proposed to improve the long-range and non-local relationship across different time-frequency locations.
- A data-independent 2D-DCT based global context model (DCT-GCT) is also proposed to improve model interpretability. A multi-DCT attention mechanism is introduced to improve the modeling power with different DCT bases.
- It is shown that the conventional GAP based SE model is a special case of attention and 2D-DCT based context models.

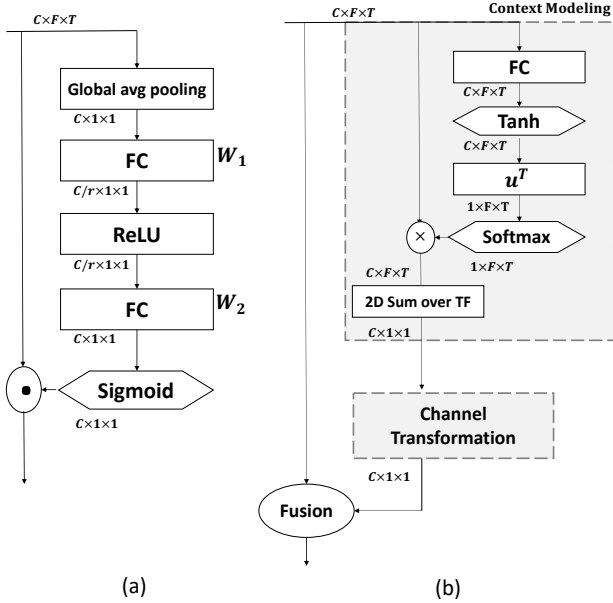


Fig. 1: (a) SE block. (b) Proposed Attention based global time-frequency context modeling framework and channel-wise transformation.

- A time-frequency enhancement (TFE) method is proposed to leverage the global context vector as an intermediate representation. It can further enhance the global context models by performing time-frequency wise recalibration.
- Finally, extensive experiments are performed to demonstrate the effectiveness of our proposed methods in both accuracy and computational complexity.

In the following sections, we review the squeeze and excitation method in Sec. II. Global time-frequency context modeling framework and the attention based context model are described in Sec. III. Sec. IV describes the 2D-DCT based context model. The time-frequency enhancement method is explained in Sec. V. We provide detailed formulation and explanations of our experiments in Sec. VIII, as well as results and discussions in Sec. IX. Finally we conclude our work in Sec. X.

II. RECAP OF SQUEEZE AND EXCITATION ATTENTION

The Squeeze and Excitation (SE) channel attention uses a squeeze operation to summarize time-frequency information into a channel embedding. This block is illustrated Fig. 1(a). We define the feature map of the input audio as $\mathbf{X} = [\mathbf{X}_1, \mathbf{X}_2, \dots, \mathbf{X}_c]$, where $\mathbf{X}_c \in \mathbb{R}^{F \times T}$ is the feature matrix of channel c . In this procedure, a global average pooling layer is applied first to generate a channel-wise embedding $\mathbf{g} \in \mathbb{R}^C$ with its c -th element,

$$g_c = \mathcal{F}_{sq}(\mathbf{X}_c) = \frac{1}{F \times T} \sum_{i=0}^{F-1} \sum_{j=0}^{T-1} \mathbf{X}_c(i, j) \quad (1)$$

This operation embeds the global time-frequency information into the intermediate output vector \mathbf{g} . This vector contains the

statistics that express of the collective time-frequency content of the input signal. In order to capture the channel wise dependencies, a gating mechanism with a sigmoid activation function is used to learn a nonlinear relationship between channels as follows,

$$\mathbf{s} = \mathcal{F}_{ex}(\mathbf{g}, \mathbf{W}) = \text{sigmoid}(\mathbf{W}_2 \text{ReLU}(\mathbf{W}_1 \mathbf{g})) \quad (2)$$

where $\mathbf{W}_1 \in \mathbb{R}^{\frac{C}{r} \times C}$ and $\mathbf{W}_2 \in \mathbb{R}^{C \times \frac{C}{r}}$ are the weights of two fully-connected layers. The dimensionality reduction factor r indicates the bottleneck in the channel excitation block. Note that the original channel dimension is recovered by the second FC layer. With a sigmoid activation function, the channel-wise attention vector \mathbf{s} is obtained. Finally U is recalibrated with the attention vector as,

$$\hat{\mathbf{X}}_c = \mathcal{F}_{scale}(\mathbf{X}_c, s_c) = s_c \cdot \mathbf{X}_c \quad (3)$$

Here, $\hat{\mathbf{X}} = [\hat{\mathbf{X}}_1, \hat{\mathbf{X}}_2, \dots, \hat{\mathbf{X}}_C]$ is the final set of channel-wise recalibrated features. In this block, the input features are attentively scaled so that the important channels are emphasized and less important ones are diminished.

III. DATA-DRIVEN ATTENTION BASED CONTEXT MODELING

The global context information and channel relationship in the SE-Net are inherently implicit. The global average operation treats each time-frequency location the same and therefore does not consider the relationship or rich information of each time-frequency bin. To better model long-range relationships and local interactions, a generalized framework is proposed based on the global context modeling for channel and time-frequency wise feature recalibration. A data-driven query-independent attention map is computed. For each time-frequency location, this attention mechanism is used to learn a weight and subsequently pool the corresponding feature values to obtain a global representation.

To summarize, an attention mechanism is first utilized to learn a global time-frequency embedding $\mathbf{g} \in \mathbb{R}^C$. Next, a channel-wise transformation is applied by broadcasting the global TF context vector to each channel. In Fig. 1(b), the process is shown on how the Global Time-Frequency Context (GTFC) embedding is learnt and applied for the channel-wise feature map enhancement: (a) the context modeling module groups the features of all positions together via global attentive pooling; (b) local channel interactions are applied next on the GTFC to capture channel-wise dependencies; (c) a fusion function is used to distribute the context vector across channels. In the following sections, further details concerning this process are described in detail.

A. Global Attention Pooling

Proposed in our prior work [65], a global context embedding module is designed to aggregate the non-local, long-range time-frequency relationship in each channel. Since individual TF locations may reflect a range of content importance for SV, an attention mechanism is used to focus on salient regions that may have more significant impact on the global context.

The module can exploit comprehensive contextual information outside the small receptive fields of the convolutional layers to better encode global TF information. Given an input feature map $\mathbf{X}_c \in \mathbb{R}^{F \times T}$, the following module is designed,

$$g_c = \sum_{i=0}^{F-1} \sum_{j=0}^{T-1} \alpha_{i,j} \mathbf{X}_c(i, j) \quad (4)$$

where $\alpha_{i,j}$ is the learned attention weight at a time-frequency location (i, j) . It is from the attention scalar score $e_{i,j}$, which is computed through an MLP \mathbf{W}_α on the feature vector $\mathbf{x}^{i,j} \in \mathbb{R}^C$ and a hidden vector \mathbf{u}_α ,

$$e_{i,j} = \mathbf{u}_\alpha^\top \tanh(\mathbf{W}_\alpha \mathbf{x}^{i,j} + \mathbf{b}) + k \quad (5)$$

where \mathbf{b} and k are bias terms. The attention score is normalized over all time-frequency locations by a softmax function so as to sum to the unity,

$$\alpha_{i,j} = \frac{\exp(e_{i,j})}{\sum_{i=0}^{F-1} \sum_{j=0}^{T-1} \exp(e_{i,j})} \quad (6)$$

The attention unit is efficient in representing the nonlinear, complex activations, and is a general form of mean or max pooling. The squeeze-excitation (SE) block is also an instantiation of our proposed framework, where $\alpha_{i,j} = \frac{1}{F \times T}$. Additionally, each time-frequency location shares one attention mask. Therefore, this query-independent attention mechanism helps efficiently learn the weight at each location to achieve a better global context representation. Since this proposed context modeling block is lightweight, it can be applied in multiple layers to capture the long-range dependency with only a slight increase in computation cost. Considering ResNet-34 as an example, ResNet-34 + Att-GCT denotes the addition of the proposed attention based global context modeling block to the last layer in ResNet-34 with a bottleneck ratio of 8. This proposed block only increases the overall system with 0.40M additional parameters.

B. Local Cross Channel Interaction

After obtaining the time-frequency context vector, it would be useful to compare two alternative ways to perform local channel interactions in order to capture the channel relationships.

- **Fully connected layer.** Same as the SE module, two FC layers are applied with dimension reduction r to reduce the model parameters. This module introduces C^2/r additional parameters, where C is the number of channels.
- **1D Convolution.** It is also possible to use 1D convolution with a kernel size of k to perform channel interactions. This operation only introduces k additional parameters. In [59], the 1D convolution operation is introduced as an Efficient Channel Attention (ECA), which is followed by an adaptive kernel size selection method, i.e., $k = \phi(C) = \lfloor \frac{\log_2(C)}{\gamma} + \frac{b}{\gamma} \rfloor$. Here, we set $\gamma = 2$ and $b = 1$ and compare with the FC layers in subsequent experiments.

Finally, we aggregate the transformed global context vector to recalibrate the feature map channel wisely with a sigmoid function and element-wise dot product operation.

IV. DATA-INDEPENDENT DCT BASED CONTEXT MODELING

In the previous section, an attention mechanism was proposed to learn the weights of each time-frequency location of the feature map. The learned weights are parametric and purely data-driven. This section further introduces a data-independent, and explainable method to compute the weights of each time-frequency location. We apply the two dimensional Discrete Cosine Transform (2D-DCT) based pooling to represent rich global context information and also show that this method is a generalized form of Global Average Pooling (GAP).

A. Discrete Cosine Transform

Given an input feature map $\mathbf{X} \in \mathbb{R}^{F \times T}$, its 2D Discrete Cosine Transform g is formulated as,

$$g_{f,t} = \sum_{i=0}^{F-1} \sum_{j=0}^{T-1} B_{f,t}^{i,j} \mathbf{X}(i, j) \quad (7)$$

where $f \in \{0, 1, \dots, F-1\}$, $t \in \{0, 1, \dots, T-1\}$, and $B_{f,t}$ is a basis function of the 2D-DCT. It is written as,

$$B_{f,t}^{i,j} = \cos\left(\frac{\pi f}{F} \left(i + \frac{1}{2}\right)\right) \cos\left(\frac{\pi t}{T} \left(j + \frac{1}{2}\right)\right) \quad (8)$$

The 2D-DCT based pooling is applied to aggregate the input feature map. The weights correspond to a specific DCT basis. For example, we visualize 64 DCT bases in Fig. 2(b). It can be proven that GAP used in SE channel attention is a special case of 2D-DCT, where f and t are set to 0. In this case, this can be written as,

$$\begin{aligned} g_{0,0} &= \sum_{i=0}^{F-1} \sum_{j=0}^{T-1} \cos\left(\frac{0}{F} \left(i + \frac{1}{2}\right)\right) \cos\left(\frac{0}{T} \left(j + \frac{1}{2}\right)\right) \mathbf{X}(i, j) \\ &= \sum_{i=0}^{F-1} \sum_{j=0}^{T-1} \mathbf{X}(i, j) \end{aligned} \quad (9)$$

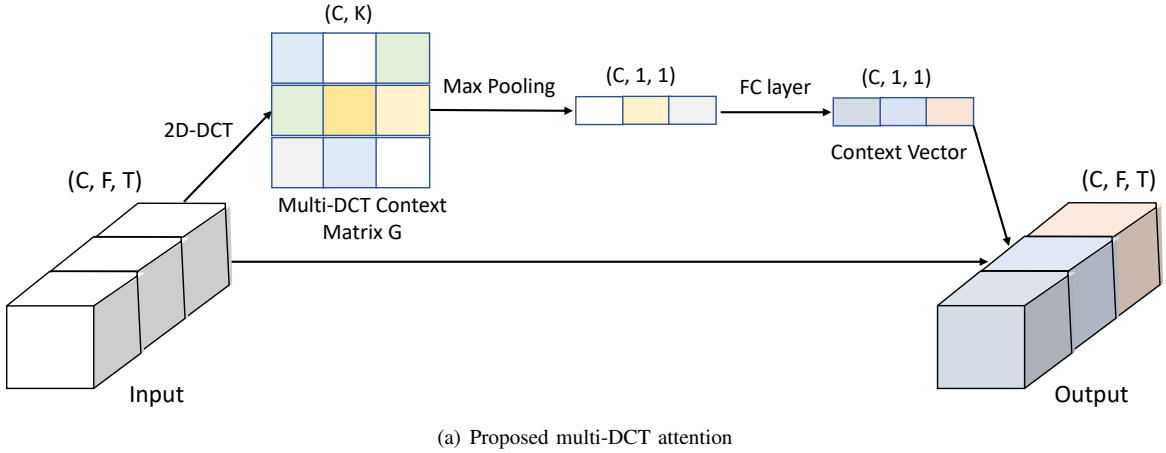
where $g_{0,0}$ represents the lowest frequency component of 2D-DCT, and it is proportional to GAP.

B. Multi-DCT Channel Attention

The previous section has shown that GAP in the SE channel attention is the lowest frequency component of 2D-DCT. In order to use rich speech information for the global context modeling, the following mechanism is designed to leverage multiple DCT components and select the maximum response for each channel. The entire process is illustrated in Fig. 2(a).

Here, denote $\mathbf{X} = [\mathbf{X}_1, \mathbf{X}_2, \dots, \mathbf{X}_c]$, where $\mathbf{X}_c \in \mathbb{R}^{F \times T}$ is the feature matrix of channel c . For one DCT component $B_{f,t}$, the corresponding 2D-DCT based global context value $g_{c,f,t}$ is written as,

$$\begin{aligned} g_{c,f,t} &= 2\text{D-DCT}^{u_i, v_i}(\mathbf{X}_c) \\ &= \sum_{i=0}^{F-1} \sum_{j=0}^{T-1} B_{f,t}^{u_i, v_i} \mathbf{X}_c(i, j) \end{aligned} \quad (10)$$



(a) Proposed multi-DCT attention

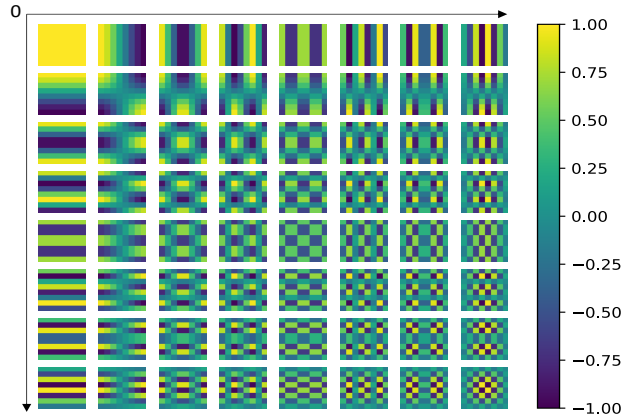
(b) An example of 8×8 DCT bases

Fig. 2: Pipeline of the proposed two-dimensional Discrete Cosine Transform based time-frequency context model.

where $[u_i, v_i]$ are the frequency component 2D indices corresponding to X_c . Therefore, for the K DCT components and each channel c , a K dimensional vector $\phi_c = [g_c^0, g_c^1, \dots, g_c^{K-1}]$ is obtained. The complete 2D-DCT global context embedding matrix can be defined as $\mathbf{G} = [\phi_0; \phi_1, \dots; \phi_c]$, where $\mathbf{G} \in \mathbb{R}^{C \times K}$. Next, a row-wise max operation is applied to select the maximum response for each channel to obtain the final global context vector $\mathbf{g} \in \mathbb{R}^C$.

$$\mathbf{g} = \max_k \mathbf{G}(:, k) \quad (11)$$

We apply the same local channel interaction and re-calibration steps discussed previously in section III-B to adjust the channel-wise feature map.

DCT component selection. Another important issue in this method is the selection process of the K DCT components. It is impractical and problematic to choose the best K DCT components with the highest performance on the test data since it requires an exhaustive set of experimental results. Essentially it's impractical to run experiments for every DCT component to create a ranked order. The ranking order also changes with different datasets. In our experiments, DCT components are pre-determined and only related to specific time and frequency indices. For instance, in Fig. 2(b), we show an example of 64 DCT components. They are ordered from (0,0) (top left), (0,1), (1,0), (1,1), ..., to (8,8) (bottom right) from the lowest

to the highest in a zigzag manner. We only select the lowest K components.

If the input feature size is fixed, we can divide the DCT space according to smallest feature map size. If input data has variable length, we can chunk the data or use adaptively average pooling to rescale the feature map to a fixed size.

V. TIME-FREQUENCY CONTENT ENHANCEMENT

We also propose a method for computing the TF attention map based on the correlation between the global TF context (GTFC) embedding and the local feature vectors. This method can further improve the proposed context models by strengthening significant time-frequency locations. In Fig. 3, we illustrate the proposed group wise time-frequency enhancement (TFE) method. First, the C channels, $F \times T$ convolutional feature map is divided into N groups along the channel dimension. It is assumed that each group could gradually learn a specific response during the training process. In each group, we have a set of local feature vectors $\mathcal{X} = \{\mathbf{x}_1, \dots, \mathbf{x}_m\}$, $\mathbf{x}_i \in \mathbb{R}^{C/N}$, $m = F \times T$. Ideally, it would be good to obtain features with strong responses at salient time-frequency positions (e.g., high energy region). However, both disturbances and reverberations may prevent us from obtaining the appropriate neuron activations following convolution. To alleviate this problem, the group-wise normalized

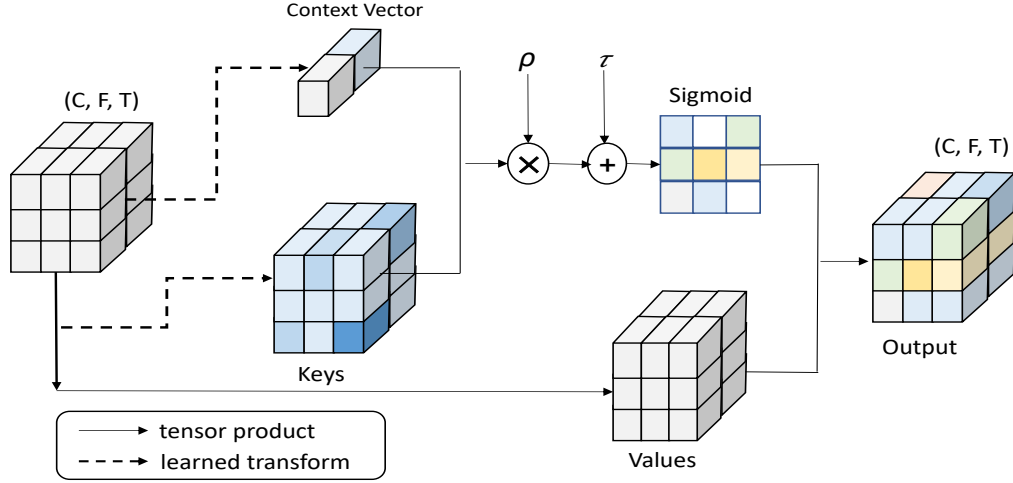


Fig. 3: Time-frequency transformation using a group-wise time-frequency interaction between the GTFC embedding and the local TF feature vector.

GTFC embedding $\hat{\mathbf{g}}$ is used as a global group representation, and the correlation is computed between the GTFC vector with the local feature vector \mathbf{x}_i at each time-frequency location. The similarity score is calculated as follows,

$$e_i = \text{score}(\hat{\mathbf{g}}, \mathbf{x}_i) = \hat{\mathbf{g}}^T \mathbf{W}_e \mathbf{x}_i \quad (12)$$

with the normalized GTFC vector $\hat{\mathbf{g}}$, we can generate the corresponding importance coefficient e_i for each position, using the general dot product scoring function [66] in Eq. (12). \mathbf{W}_e is a weight matrix to be learned. Additionally, e needs to be normalized over the time-frequency domain to prevent the biased magnitude of coefficients between various samples,

$$\hat{e}_i = \frac{e_i - \mu_e}{\sigma_e + \epsilon}, \mu_e = \frac{1}{m} \sum_{j=1}^m e_j, \sigma_e^2 = \frac{1}{m} \sum_{j=1}^m (e_j - \mu_e)^2 \quad (13)$$

where ϵ (e.g., $1e-5$) is a constant for numerical stability. We provide a pair of parameters (ρ, τ) for each coefficient e_i to ensure that the normalization introduced in the network can represent the identity transformation. The parameters scale and shift the normalized value. Finally, to obtain the enhanced feature vector $\hat{\mathbf{x}}_i$, the original \mathbf{x}_i is scaled by the generated importance coefficients via a sigmoid function σ over the space as follows,

$$s_i = \rho \hat{e}_i + \tau \quad (14)$$

$$\hat{\mathbf{x}}_i = \mathbf{x}_i \cdot \sigma(s_i) \quad (15)$$

The recalibrated new feature group has all of the enhanced features. It is worth noting that the total number of ρ and τ is equal to the number of groups, which is negligible compared to the millions of model parameters.

VI. SPEAKER RECOGNITION MODEL

A. Model Structure

In this study, ResNet34 is used as our speaker recognition model. It is widely used in the speaker recognition community. The residual layers' channel sizes are 16, 32, 64, and 128, respectively, representing half of a standard ResNet34 model.

Attentive statistical pooling [27] is applied to aggregate the variable-length input sequence into a fixed utterance-level speaker embedding. For the loss function, the softmax and angular prototypical loss [10] are combined to learn discriminative embeddings.

B. Loss Function

To learn discriminative speaker embeddings, for each mini-batch, M utterances are sampled from every speaker. The prototype of the speaker is defined as,

$$\mathbf{c}_j = \frac{1}{M-1} \sum_{m=1}^{M-1} \mathbf{x}_{j,m} \quad (16)$$

During training, each example is classified against N speakers based on a softmax over distances to each speaker prototype, the angular prototypical loss with learnable scale and bias is represented as,

$$L_p = -\frac{1}{N} \sum_{j=1}^N \log \frac{e^{w \cdot \cos(\mathbf{x}_{j,M}, \mathbf{c}_j) + b}}{\sum_{k=1}^N e^{w \cdot \cos(\mathbf{x}_{j,M}, \mathbf{c}_k) + b}} \quad (17)$$

The number of utterances per speaker M is set to 2 in our experiments. For the classification purpose, a multi-class softmax cross-entropy loss is used as follows,

$$L_s = -\frac{1}{N} \sum_{i=1}^N \log \frac{e^{\mathbf{W}_{y_i}^T \mathbf{x}_i + b_{y_i}}}{\sum_{j=1}^C e^{\mathbf{W}_j^T \mathbf{x}_i + b_j}} \quad (18)$$

where W and b are the weight and bias of the last FC layer. The angular prototypical loss and the cross-entropy loss are combined as our speaker loss function $L = L_s + L_p$.

C. Implementation Details

It is known that system settings vary a lot for many speaker recognition solutions. Performance improvement in some studies may actually come from other modules such as data augmentation. For a fair comparison and evaluation for

our proposed methods alone, we follow the data augmentation, and model backbone in a well-known study [67]. An AdamW [68] optimizer is used with $5e-5$ weight decay. A linear warmup strategy is applied for the first 5 epochs to the initial learning rate 10^{-3} . The learning rate is reduced by 0.75 every 18 epochs. The extracted utterance-level embeddings are L2 normalized, and the dimension size is 512. The general dot-product scoring function is applied to compute the time-frequency attention matrix. The proposed global context model block is inserted after the last Batch Norm layer in each residual basic block. Also, cosine distance scoring is applied to evaluate verification performance. We sample 2 utterances per speaker for each mini-batch, and 500 utterances per speaker for each epoch.

VII. CORPORA

For this study, the VoxCeleb 1 and 2 [69], [70] datasets are used for experiments. Models are trained on Voxceleb1 dev set and Voxceleb2 dev set, respectively. Voxceleb1 dev is used to train the base models for ablation studies and analysis of model structure and parameters. Voxceleb2 dev is used to train our final models. Voxceleb1 dev set contains 148,642 utterances from 1211 celebrities, and Voxceleb2 dev set has 5994 speakers with 1,092,009 utterances. Both are large scale datasets extracted from YouTube videos that are recorded across a large number of challenging visual and auditory environments, including background conversations, laughter, overlapping speech, and a wide range of varying room acoustics. To evaluate performance of the proposed global time-frequency context models for speaker representation learning, we test our models on three trial lists: (1) VoxCeleb 1-O: original trial list containing 37,611 trials from 40 speakers in the Voxceleb 1 test set; (2) Voxceleb 1-E: extended trial list containing 579,818 trials from 1251 speakers; and (3) Voxceleb 1-H: hard trial list containing 550,894 trials from 1190 speakers.

VIII. EXPERIMENTS

A. Feature Extraction

We compute 64 dimensional log-mel filter-bank energies (fbank) at the frame level as input features. A Hamming window of length 25 ms with 10 ms frame shift is used to extract fbanks from input audio signals. A chunk of 200 frames features of each audio file are used as input to the network. The input features are mean normalized at the frame level.

B. Data Augmentation

The original data is augmented on the fly with noise and room impulse response (RIR) from the MUSAN [71] and OpenSLR Room Impulse Response and Noise [72] corpora. There are in total 60 hours of human speech, 42 hours of music, and 6 hours of other background noise types in the MUSAN corpus. The reverberation and noise data simulation is randomly selected with equal probability. For each augmentation, one noise file is randomly selected from the MUSAN database and added to the recording with 0-15 dB

SNR. Alternatively, one music file is randomly selected from the same database and added to the recording with 5-15 dB SNR. Human babble speech is selected with 13-20 dB SNR. Otherwise, a reverberation file is selected from the RIR dataset.

C. Evaluation Metric

Performance is reported in terms of Equal Error Rate (EER), where the false accept rate and false reject rate are equal, as well as the minimum Detection Cost Function (minDCF) with settings $P_{target} = 0.01, C_{miss} = 1, C_{fa} = 1$.

IX. RESULTS AND DISCUSSIONS

A. Experimental Results

In order to thoroughly evaluate our proposed methods, we compare all proposed models and later show a detailed ablation analysis. Experiments are first performed on the attention based global context model (Att-GCT), followed by the group-wise time-frequency enhancement (Att-GCT-TFE), and then the DCT based global context model (DCT-GCT) for speaker verification. Finally, we show the analysis of various factors that may affect the performance of the proposed global context models.

A strong backbone ResNet34 model is used with ASP pooling, along with the loss function explained in Sec. VI-B. This achieves 2.45% EER and 0.3471 minDCF using only the Voxceleb1 dev set. The baseline Squeeze and Excitation module can recalibrate each channel of the speech feature map to emphasize important channels and diminish insignificant ones. The computational cost of the SE module is on the order of $O(C^2/r)$, where C is the number of channels and r (16 in our experiments) is the reduction ratio used to reduce the model parameters. As shown in Table II, the SE module brings 3.27% relative improvement in EER. This indicates that context modeling (GAP) and channel interactions are helpful to learn a good speaker embedding.

Channel Transform As discussed in Sec. III-B, for the proposed Att-GCT model, two channel transform modules are first compared in Table I. The ECA module only has k (kernel size of 1D Conv) extra parameters, and is an effective option if a compact model is needed for on-device applications. The FC layer, however, achieves the best result. It brings extra C^2/r parameters. For the best performance purpose, in all subsequent experiments, two FC layer are used as the channel transform with $r = 16$.

TABLE I
EMPIRICAL ANALYSIS FOR DIFFERENT CHANNEL TRANSFORMS OF THE ATT-GCT BLOCK.

Channel transform	EER(%)	minDCF	Train Set
FC layer	2.16	0.2768	VoxCeleb1
ECA	2.24	0.3044	VoxCeleb1

Table II shows all results for our proposed models with the best settings. For the attention based context model, the proposed channel wise attention (Att-GCT) improves SV performance by a large margin compared with the ResNet34 model. With the Att-GCT block, overall EER of the ResNet34

model decreases from 2.45% to 2.16%, relatively 11.84%. Also, a relative reduction of 8.86% EER is achieved compared with the SE block. These results may suggest that our proposed attention based global time-frequency context block can greatly recalibrate the significant feature regions to improve speaker verification performance with the context information.

TABLE II
SV RESULTS ON THE VOXCeleb1-O TEST SET USING VARIOUS MODELS AND OUR PROPOSED GLOBAL TIME FREQUENCY CONTEXT BLOCKS.

Model	EER (%)	minDCF	Train Set
Ivector [69]	8.80	0.7300	VoxCeleb1
Xvector [27]	3.85	0.4060	VoxCeleb1
SPE [29]	4.20	0.4220	VoxCeleb1
LDE [30]	4.56	0.4410	VoxCeleb1
MHSA [28]	4.00	0.4500	VoxCeleb1
ResNet34	2.45	0.3471	VoxCeleb1
ResNet34 + SE	2.37	0.3570	VoxCeleb1
ResNet34 + Att-GCT (ours)	2.16	0.2768	VoxCeleb1
ResNet34 + Att-GCT + TFE (ours)	2.10	0.2602	VoxCeleb1
ResNet34 + DCT-GCT (ours)	2.13	0.2503	VoxCeleb1
ResNet34 + DCT-GCT + TFE (ours)	2.07	0.2552	VoxCeleb1

Consistent performance improvement is also observed with time-frequency enhancement step (Att-GCT-TFE). The EER reduces from 2.16% to 2.10%, with an additional relative 2.78% improvement. It is suggested that with a good intermediate global context representation, it is possible to use the interaction between local information at each time-frequency location and global context information to adjust the speech representations. By emphasizing time-frequency important features and ignoring irrelevant features, this solution obtains more meaningful information for SID compared with calibrating channel-wise features alone.

For the DCT based context model, it is observed that 2D-DCT coefficients specific to a the time-frequency location are informative for context modeling. The number of additional parameters introduced with this module is 0 since all DCT coefficients are pre-computed. Here, fixed length 200 frames of 64-dim fbank are used as input features, the 2D-DCT space is divided into 8×25 parts since the smallest feature map size after the last block is 8×25 .

With this method, there is a relative reduction of 10.13% and 12.66% EER when comparing SE with DCT-GCT and DCT-GCT-TFE respectively. This indicates that GAP does not reflect sufficient information from each time-frequency location, while the results of DCT context models are as effective as the attention context models. Another advantage is that the weights are pre-computed. Based on the observations, further detailed analysis will be presented in Sec. IX-C.

B. Analysis of Attention Context Model

In this section, further analysis is presented regarding factors that may affect performance of the attention context model with the TFE block.

Normalization components ρ and τ . As shown in Table III, the initialization of normalization parameters ρ and τ in the Att-GCT-TFE block affects the verification results. Initializing ρ to 0 tends to give better results. With a grid search, it is

determined that the best setting is to assign ρ to 0 and τ to 1. This suggests that it is appropriate to discard the context-guided time-frequency enhancement in the very early stage of network training. It is meaningful to firstly learn a good representation with the convolution stem.

TABLE III
EMPIRICAL ANALYSIS FOR NORMALIZATION PARAMETERS OF THE ATT-GCT-TFE METHOD.

(ρ, τ)	EER (%)	minDCF	Train set
(0, 0)	2.13	0.2725	VoxCeleb1
(0, 1)	2.10	0.2602	VoxCeleb1
(1, 0)	2.26	0.2867	VoxCeleb1
(1, 1)	2.32	0.3110	VoxCeleb1

Group number. We further investigate the number of groups in the Att-GCT-TFE module in Table IV. A limited number of groups may cause the diversity of feature representations to be limited. Using the group number 8, we obtain the best EER and DCF values. Too many groups result in a dimension reduction in the feature space, which may cause a weaker representation for each group response. The group number is set to 8 in all our experiments.

TABLE IV
EMPIRICAL ANALYSIS FOR GROUP NUMBER OF THE ATT-GCT-TFE METHOD.

Group number	EER (%)	minDCF	Train Set
4	2.34	0.3003	VoxCeleb1
8	2.10	0.2602	VoxCeleb1
16	2.16	0.2699	VoxCeleb1

Block position. As shown in Table V, inserting the proposed module after/before the Batch Norm layer, or before the convolution layer in the Residual basic block all improves the results, compared with baseline ResNet34 and SE model. Here, only one proposed block is inserted after the Batch Norm layer in our experiments. The Att-GCT-TFE block only requires about 0.40M additional parameters, and therefore is very computationally efficient.

TABLE V
EMPIRICAL ANALYSIS FOR THE BLOCK POSITION OF THE ATT-GCT-TFE METHOD.

Block position	EER (%)	minDCF	Train Set
after BN	2.10	0.2602	VoxCeleb1
before BN	2.29	0.2865	VoxCeleb1
before Conv	2.32	0.3183	VoxCeleb1

C. Analysis of DCT Context Model

As noted in Sec. IV-B, the K lowest DCT components are chosen as the bases. Here we compare [1,2,4,8,16,32] lowest frequency components and show the result in Table VI. 1 DCT basis corresponds to the original GAP in the channel attention. In this case, all other DCT components are discarded. It is noted with frequency components and a maximum activation function, it is possible to embed more time-frequency information into one channel. When using 2 DCT components, our

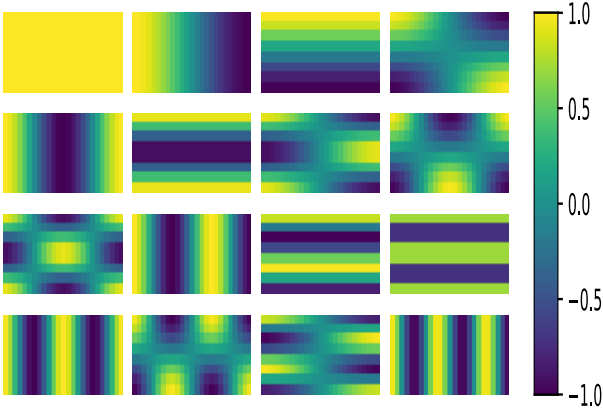


Fig. 4: Visualization of the lowest 16 DCT components of the 8×25 DCT bases, order from 1st lowest to the 16th lowest along the row dimension. The first two are the two lowest DCT components used in our models.

model obtains the best result with a 2.13% EER and 0.25 DCF, which is relatively 10.13% and 29.89% lower than GAP. Also, when two channels are redundant in the speech representation, we may obtain the same information using GAP. However, in the proposed multi-DCT attention framework, we can get more information since different frequency components can be selected. The number of frequency components is set to 2 in all our experiments.

TABLE VI
SV RESULTS ON THE VOXCELEB1 TEST SET USING THE DCT-GCT METHOD

Number	EER (%)	minDCF	Train Set
1	2.37	0.3570	VoxCeleb1
2	2.13	0.2503	VoxCeleb1
4	2.27	0.3110	VoxCeleb1
8	2.23	0.2813	VoxCeleb1
16	2.23	0.2914	VoxCeleb1
32	2.32	0.3236	VoxCeleb1

D. Visualization of Selected DCT Components

In Fig. 4, we show the 16 lowest DCT base functions of 8×25 DCT parts. These are ordered from the 1st to 16th lowest along the row. The figure shows that 2D DCT basis functions are composed of regular horizontal and vertical cosine wave functions. These DCT components are orthogonal and data-independent. The DCT based global context model largely improves model explainability and efficiency. Compared with attention based global context model, all DCT weights are pre-computed. Therefore, overall model complexity is significantly reduced. The first two components in the first row are the two lowest components, which are used in all our experiments for DCT based context models.

E. Duration Analysis

Next, in Fig. 5, performance of the four systems are shown over a range of test data durations. In general, performance

degrades when the test data duration becomes smaller. Especially in very short test conditions, it is very challenging to maintain effective performance. In terms of EER, attention and DCT based global context models are more robust for short duration data compared with SE model. When duration is very short (e.g., 1s), context models and SE are all vulnerable. From ResNet34 to ResNet34+SE system, there is an average of 6.77% relative improvement in EER across different durations. The Att-GCT and DCT-GCT context models obtain additional 13.97% and 15.19% improvement on average, respectively. Also, a high false rejection rate means that the same speakers are incorrectly classified since they are very near in the cosine distance space. This suggests that if it is possible to further improve discriminative ability in the speaker embedding, (e.g., by introducing more utterances per speaker or adding more augmentation), there is still room to improve performance. Deduced from Fig. 5, in most occasions, speaker recognition systems are vulnerable when test data are too short. It would be better to filter out very short data when performing data collection in real scenarios. It also suggests that our speaker model might learn more meaningful information with global context modules and reduce the impact of duration mismatch. The proposed systems might be helpful in some very short duration speaker or keyword detection applications.

F. Results with Models Trained on Voxceleb2 Data

Based on comprehensive analysis and ablation studies in previous sections, we show the results of our best proposed models trained on the Voxceleb2 dev split, and compare with other public results. Methods such as E-TDNN [20], [21] and ARET [22] are based on Time-Delay Neural Network (TDNN). ft-CBAM [45] (re-implemented following the original paper) is based on ResNet34. From Table VII, it can be observed that a significant improvement with our proposed attention and DCT based context models is achieved. Compared with the baseline SE block, there is an average of 10.21% relative improvement in EER over three test trials using the attention context model Att-GCT-TFE, and 12.38% relative improvement using the DCT context model DCT-GCT-TFE. Results of DCT based global context model are as good as attention based context model. The difference that is DCT coefficients are pre-computed with no increase in computational costs. With these two convenient modules, our approach can easily improve speaker recognition performance by emphasizing important regions. It not only essentially saves computational costs but also improves model interpretability. The attention context model is purely data driven, so it may obtain better performance at some conditions by emphasizing salient regions. It does not require additional DCT component selection or a mapping between the feature map and the DCT indices either.

X. CONCLUSIONS

In this study, a global time-frequency context modeling framework has been proposed and successfully applied to the both channel and time-frequency wise feature map recalibration. Our proposed global context models mainly include

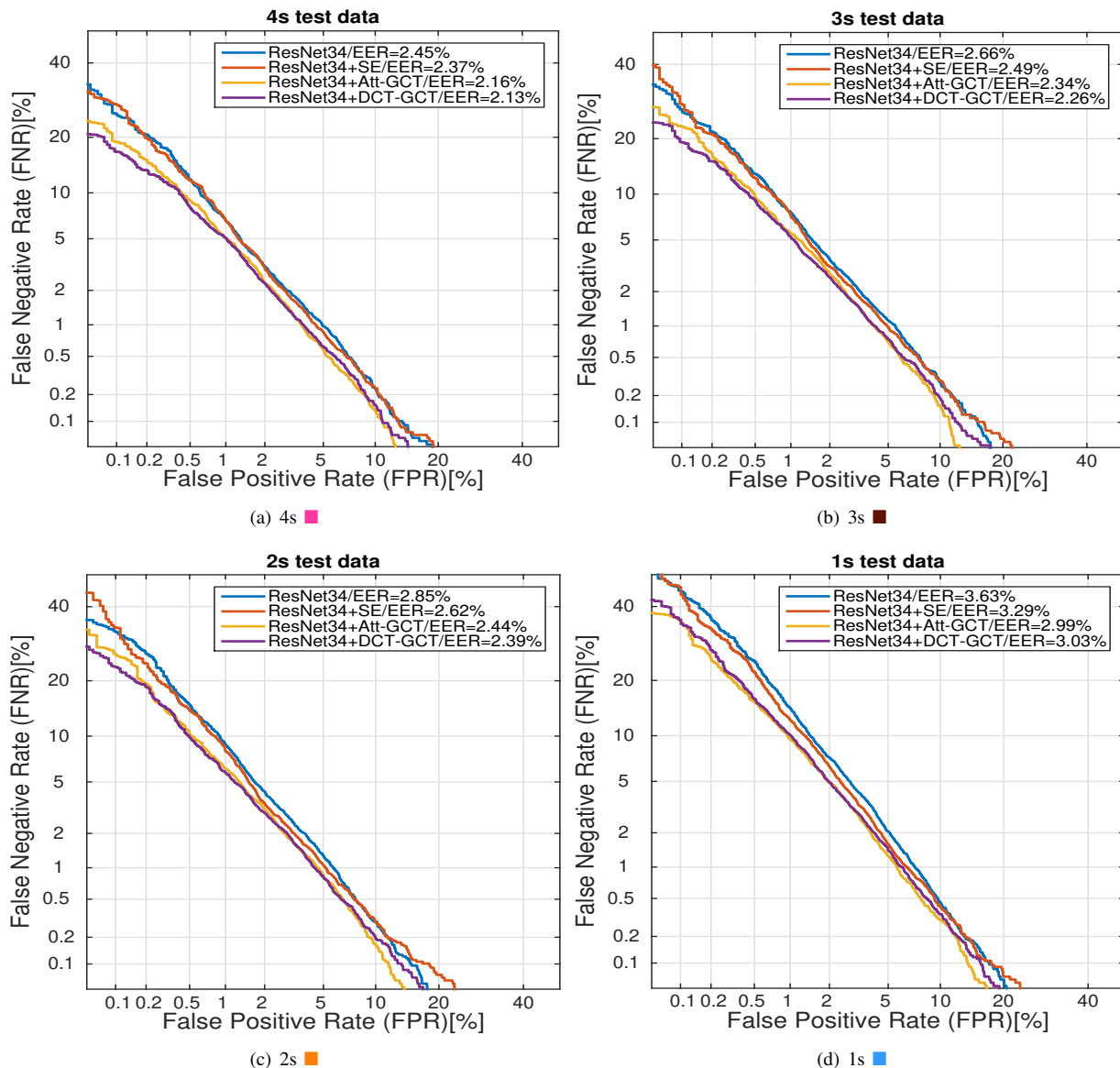


Fig. 5: Detection Error Trade-off (DET) curves for each system on different test data duration - 4, 3, 2, 1s respectively.

data-driven attention-based and data-independent DCT based context models. A time-frequency enhancement method was also proposed to leverage the correlation between global context and local feature vectors at each time-frequency to better guide the speaker representation learning. The attention context model can capture long-range time-frequency dependency and channel variances. This lightweight block was shown to enhance the latent speaker representation and suppress possible distortions. The block was inserted after the last Batch Norm layer of each Residual basic block. The DCT context model used the pre-computed DCT coefficients as weights. A multi-DCT approach was proposed to use different DCT components. The solution also illustrated that GAP in SE is a special case of the formulated attention and DCT based context models. Experimental results were significantly improved by emphasizing the import channel and time-frequency regions with our proposed methods.

Extensive experiments, ablation studies, and analysis were performed to evaluate the proposed methods on Voxceleb data. The approaches were shown to improve the ResNet and SE models in terms of both EER and DCF by a large margin. We found that FC layer used for channel transformation obtained the best result compared with 1D Conv. For on-device applications, choosing 1D Conv with a small kernel size K would be worthwhile since it can reduce the additional parameters introduced by channel transform from an order of $O(C^2/r)$ to $O(K)$. The time-frequency enhancement method can further improve the proposed context models by strengthening significant time-frequency locations. We also discussed the various impact of the normalization components, group number, and block position on the Att-GCT-TFE method. For our proposed DCT context models, we found that we could get more information with multiple DCT components. It is suggested to use the two lowest frequency components with

TABLE VII

SV RESULTS ON THE VOXCELEB1 TEST SET USING MODELS WITH OUR PROPOSED GLOBAL TIME FREQUENCY CONTEXT BLOCKS. SPEAKER MODELS ARE TRAINED ON THE VOXCELEB2 DEV SPLIT.

Model	VoxCeleb1-O		VoxCeleb1-E		VoxCeleb1-H		Train set
	EER (%)	minDCF	EER (%)	minDCF	EER (%)	minDCF	
E-TDNN [21]	1.49	0.1604	1.61	0.1712	2.69	0.2419	Voxceleb2
ARET-25 [22]	1.39	N/A	1.52	N/A	2.61	N/A	Voxceleb2
CBAM [45]	1.06	0.1255	1.24	0.1562	2.49	0.2562	Voxceleb2
ResNet34 + SE	1.10	0.1254	1.22	0.1556	2.40	0.2693	Voxceleb2
ResNet34 + Att-GCT (ours)	0.98	0.1186	1.14	0.1452	2.26	0.2482	Voxceleb2
ResNet34 + Att-GCT-TFE (ours)	0.94	0.1075	1.10	0.1406	2.25	0.2407	Voxceleb2
ResNet34 + DCT-GCT (ours)	0.97	0.1143	1.12	0.1430	2.28	0.2494	Voxceleb2
ResNet34 + DCT-GCT-TFE (ours)	0.90	0.1036	1.08	0.1392	2.22	0.2410	Voxceleb2

the proposed method. The proposed global context models not only achieve better performance compared with the SE block, but also are more robust to short duration test data in general. They might also be helpful for short duration speaker or keyword detection applications.

The proposed global context models can effectively recalibrate the feature maps adaptively by emphasizing more important channels and time-frequency locations. For future work, it is suggested to consider adjusting the framework and perform attention on the frequency dimension. At the same time, this approach might be applied to many other applications such as language identification, speaker adaption for speech recognition, spoofing detection, emotion or stress recognition, etc. Therefore, this study highlights effective global context methods for text-independent speaker recognition and fundamental observations for future studies.

REFERENCES

- [1] P. Foggia, N. Petkov, A. Saggese, N. Strisciuglio, and M. Vento, "Audio surveillance of roads: A system for detecting anomalous sounds," *IEEE transactions on intelligent transportation systems*, vol. 17, no. 1, pp. 279–288, 2016.
- [2] K. A. Lee, A. Larcher, H. Thai, B. Ma, and H. Li, "Joint application of speech and speaker recognition for automation and security in smart home," in *Twelfth Annual Conference of the International Speech Communication Association*, 2011.
- [3] M. Crocco, M. Cristani, A. Trucco, and V. Murino, "Audio surveillance: A systematic review," *ACM Computing Surveys (CSUR)*, vol. 48, no. 4, p. 52, 2016.
- [4] Q. Wang, H. Muckenhirn, K. Wilson, P. Sridhar, Z. Wu, J. R. Hershey, R. A. Saurous, R. J. Weiss, Y. Jia, and I. L. Moreno, "Voicefilter: Targeted voice separation by speaker-conditioned spectrogram masking," *Proc. Interspeech 2019*, pp. 2728–2732, 2019.
- [5] J. Xie, L. P. Garcia-Perera, D. Povey, and S. Khudanpur, "Multi-plda diarization on children's speech," in *Interspeech*, 2019, pp. 376–380.
- [6] S.-J. Chen, W. Xia, and J. H. Hansen, "Scenario aware speech recognition: Advancements for apollo fearless steps & chime-4 corpora," in *IEEE Automatic Speech Recognition and Understanding Workshop (ASRU)*, 2021, pp. 289–295.
- [7] D. Yu, M. Kolbæk, Z.-H. Tan, and J. Jensen, "Permutation invariant training of deep models for speaker-independent multi-talker speech separation," in *2017 IEEE International Conference on Acoustics, Speech and Signal Processing (ICASSP)*. IEEE, 2017, pp. 241–245.
- [8] J. Lau, B. Zimmerman, and F. Schaub, "Alexa, are you listening? privacy perceptions, concerns and privacy-seeking behaviors with smart speakers," *Proceedings of the ACM on Human-Computer Interaction*, vol. 2, no. CSCW, pp. 1–31, 2018.
- [9] F. R. rahman Chowdhury, Q. Wang, I. L. Moreno, and L. Wan, "Attention-based models for text-dependent speaker verification," in *2018 IEEE International Conference on Acoustics, Speech and Signal Processing (ICASSP)*. IEEE, 2018, pp. 5359–5363.
- [10] J. S. Chung, J. Huh, S. Mun, M. Lee, H.-S. Heo, S. Choe, C. Ham, S. Jung, B.-J. Lee, and I. Han, "In defence of metric learning for speaker recognition," *Proc. Interspeech 2020*, pp. 2977–2981, 2020.
- [11] W. Xia, J. Huang, and J. H. Hansen, "Cross-lingual text-independent speaker verification using unsupervised adversarial discriminative domain adaptation," in *IEEE International Conference on Acoustics, Speech and Signal Processing (ICASSP)*. IEEE, 2019, pp. 5816–5820.
- [12] L. Wan, Q. Wang, A. Papir, and I. L. Moreno, "Generalized end-to-end loss for speaker verification," in *Acoustics, Speech and Signal Processing (ICASSP), IEEE International Conference on*, 2018, pp. 4879–4883.
- [13] C. Zhang, K. Koishida, and J. H. Hansen, "Text-independent speaker verification based on triplet convolutional neural network embeddings," *IEEE/ACM Transactions on Audio, Speech and Language Processing (TASLP)*, vol. 26, no. 9, pp. 1633–1644, 2018.
- [14] E. Variani, X. Lei, E. McDermott, I. L. Moreno, and J. Gonzalez-Dominguez, "Deep neural networks for small footprint text-dependent speaker verification," in *2014 IEEE international conference on acoustics, speech and signal processing (ICASSP)*. IEEE, 2014, pp. 4052–4056.
- [15] P. Matějka, O. Glembek, F. Castaldo, M. J. Alam, O. Plchot, P. Kenny, L. Burget, and J. Černocký, "Full-covariance ubm and heavy-tailed plda in i-vector speaker verification," in *Acoustics, Speech and Signal Processing (ICASSP), IEEE International Conference on*, 2011, pp. 4828–4831.
- [16] J. H. Hansen and T. Hasan, "Speaker recognition by machines and humans: A tutorial review," *IEEE Signal processing magazine*, vol. 32, no. 6, pp. 74–99, 2015.
- [17] P. Kenny, "Bayesian speaker verification with heavy-tailed priors." in *Odyssey*, 2010, p. 14.
- [18] S. J. Prince and J. H. Elder, "Probabilistic linear discriminant analysis for inferences about identity," in *Computer Vision (ICCV), IEEE International Conference on*, 2007, pp. 1–8.
- [19] D. Snyder, D. Garcia-Romero, G. Sell, D. Povey, and S. Khudanpur, "X-vectors: Robust dnn embeddings for speaker recognition," in *2018 IEEE International Conference on Acoustics, Speech and Signal Processing (ICASSP)*. IEEE, 2018, pp. 5329–5333.
- [20] D. Snyder, D. Garcia-Romero, G. Sell, A. McCree, D. Povey, and S. Khudanpur, "Speaker recognition for multi-speaker conversations using x-vectors," in *IEEE International conference on acoustics, speech and signal processing (ICASSP)*, 2019, pp. 5796–5800.
- [21] B. Desplanques, J. Thienpondt, and K. Demuynck, "Ecapa-tdnn: Emphasized channel attention, propagation and aggregation in tdnn based speaker verification," *Proc. Interspeech 2020*, pp. 3830–3834, 2020.
- [22] R. Zhang, J. Wei, W. Lu, L. Wang, M. Liu, L. Zhang, J. Jin, and J. Xu, "Aret: Aggregated residual extended time-delay neural networks for speaker verification," in *INTERSPEECH*, 2020, pp. 946–950.
- [23] W. Liu, Y. Wen, Z. Yu, M. Li, B. Raj, and L. Song, "Sphereface: Deep hypersphere embedding for face recognition," in *Proceedings of the IEEE conference on computer vision and pattern recognition*, 2017, pp. 212–220.
- [24] F. Wang, J. Cheng, W. Liu, and H. Liu, "Additive margin softmax for face verification," *IEEE Signal Processing Letters*, vol. 25, no. 7, pp. 926–930, 2018.
- [25] J. Deng, J. Guo, N. Xue, and S. Zafeiriou, "Arcface: Additive angular margin loss for deep face recognition," in *Proceedings of the IEEE Conference on Computer Vision and Pattern Recognition*, 2019, pp. 4690–4699.

- [26] Z. Wang, Y. Wang, B. Dong, S. Pracheta, K. Hamlen, and L. Khan, "Adaptive margin based deep adversarial metric learning," in *2020 IEEE 6th Intl Conference on Big Data Security on Cloud (BigDataSecurity), IEEE Intl Conference on High Performance and Smart Computing (HPSC) and IEEE Intl Conference on Intelligent Data and Security (IDS)*. IEEE, 2020, pp. 100–108.
- [27] K. Okabe, T. Koshinaka, and K. Shinoda, "Attentive statistics pooling for deep speaker embedding," *Proc. Interspeech 2018*, pp. 2252–2256, 2018.
- [28] M. India, P. Safari, and J. Hernando, "Self multi-head attention for speaker recognition," *Proc. Interspeech 2019*, pp. 4305–4309, 2019.
- [29] Y. Jung, Y. Kim, H. Lim, Y. Choi, and H. Kim, "Spatial pyramid encoding with convex length normalization for text-independent speaker verification," *Proc. Interspeech 2019*, pp. 4030–4034, 2019.
- [30] W. Cai, J. Chen, and M. Li, "Exploring the encoding layer and loss function in end-to-end speaker and language recognition system," in *Proc. Odyssey 2018 The Speaker and Language Recognition Workshop*, 2018, pp. 74–81.
- [31] V. Kothapally and J. H. L. Hansen, "Skipconvgan: Monaural speech dereverberation using generative adversarial networks via complex time-frequency masking," *IEEE/ACM Transactions on Audio, Speech, and Language Processing*, vol. 30, pp. 1600–1613, 2022.
- [32] N. Mamun, R. Ghosh, and J. H. Hansen, "Quantifying cochlear implant users' ability for speaker identification using ci auditory stimuli," *Proc. Interspeech 2019*, pp. 3118–3122, 2019.
- [33] A. Joglekar and J. H. Hansen, "Fearless steps, nasa's first heroes: Conversational speech analysis of the apollo-11 mission control personnel," *The Journal of the Acoustical Society of America*, vol. 146, no. 4, pp. 2956–2956, 2019.
- [34] J.-w. Jung, H.-S. Heo, J.-h. Kim, H.-j. Shim, and H.-J. Yu, "Rawnet: Advanced end-to-end deep neural network using raw waveforms for text-independent speaker verification," *Proc. Interspeech 2019*, pp. 1268–1272, 2019.
- [35] H.-s. Heo, J.-w. Jung, I.-h. Yang, S.-h. Yoon, and H.-j. Yu, "Joint Training of Expanded End-to-End DNN for Text-Dependent Speaker Verification," in *INTERSPEECH*, 2017, pp. 1532–1536.
- [36] Z. Wang, W. Xia, and J. H. Hansen, "Cross-domain adaptation with discrepancy minimization for text-independent forensic speaker verification," *Proc. Interspeech 2020*, pp. 2257–2261, 2020.
- [37] Z. Wang and J. H. Hansen, "Multi-source domain adaptation for text-independent forensic speaker recognition," *IEEE/ACM Transactions on Audio, Speech, and Language Processing*, vol. 30, pp. 60–75, 2021.
- [38] J. Hu, L. Shen, and G. Sun, "Squeeze-and-excitation networks," in *Proceedings of the IEEE conference on computer vision and pattern recognition*, 2018, pp. 7132–7141.
- [39] I. Bello, B. Zoph, A. Vaswani, J. Shlens, and Q. V. Le, "Attention augmented convolutional networks," in *Proceedings of the IEEE International Conference on Computer Vision*, 2019, pp. 3286–3295.
- [40] Y. Cao, J. Xu, S. Lin, F. Wei, and H. Hu, "Gcnet: Non-local networks meet squeeze-excitation networks and beyond," in *ICCV Workshops*, 2019.
- [41] L. Zhang, Q. Wang, and L. Xie, "Duality temporal-channel-frequency attention enhanced speaker representation learning," in *ASRU*. IEEE, 2021, pp. 206–213.
- [42] W. Xia and J. H. Hansen, "Speaker representation learning using global context guided channel and time-frequency transformations," *Proc. Interspeech 2020*, pp. 3226–3230, 2020.
- [43] W. Xia and K. Koishida, "Sound event detection in multichannel audio using convolutional time-frequency-channel squeeze and excitation," *Proc. Interspeech 2019*, pp. 3629–3633, 2019.
- [44] S. Woo, J. Park, J.-Y. Lee, and I. So Kweon, "Cbam: Convolutional block attention module," in *Proceedings of the European Conference on Computer Vision (ECCV)*, 2018, pp. 3–19.
- [45] S. Yadav and A. Rai, "Frequency and temporal convolutional attention for text-independent speaker recognition," in *ICASSP*. IEEE, 2020, pp. 6794–6798.
- [46] J. Fu, J. Liu, H. Tian, Y. Li, Y. Bao, Z. Fang, and H. Lu, "Dual attention network for scene segmentation," in *Proceedings of the IEEE/CVF conference on computer vision and pattern recognition*, 2019, pp. 3146–3154.
- [47] J. Dai, H. Qi, Y. Xiong, Y. Li, G. Zhang, H. Hu, and Y. Wei, "Deformable convolutional networks," in *Proceedings of the IEEE international conference on computer vision*, 2017, pp. 764–773.
- [48] Q. Hou, D. Zhou, and J. Feng, "Coordinate attention for efficient mobile network design," in *Proceedings of the IEEE/CVF Conference on Computer Vision and Pattern Recognition*, 2021, pp. 13 713–13 722.
- [49] X. Wang, R. Girshick, A. Gupta, and K. He, "Non-local neural networks," in *Proceedings of the IEEE conference on computer vision and pattern recognition*, 2018, pp. 7794–7803.
- [50] Q. Wang, B. Wu, P. Zhu, P. Li, W. Zuo, and Q. Hu, "Eca-net: Efficient channel attention for deep convolutional neural networks," in *CVPR*.
- [51] X. Li, W. Wang, X. Hu, and J. Yang, "Selective kernel networks," in *CVPR*, 2019, pp. 510–519.
- [52] H. Zhang, C. Wu, Z. Zhang, Y. Zhu, H. Lin, Z. Zhang, Y. Sun, T. He, J. Mueller, R. Manmatha *et al.*, "Resnest: Split-attention networks," *arXiv preprint arXiv:2004.08955*, 2020.
- [53] Z. Wang, S. Gupta, J. Hao, X. Fan, D. Li, A. H. Li, and C. Guo, "Contextual rephrase detection for reducing friction in dialogue systems," in *Proceedings of the 2021 Conference on Empirical Methods in Natural Language Processing*, 2021, pp. 1899–1905.
- [54] W. Han, Z. Zhang, Y. Zhang, J. Yu, C.-C. Chiu, J. Qin, A. Gulati, R. Pang, and Y. Wu, "Contextnet: Improving convolutional neural networks for automatic speech recognition with global context," *Proc. Interspeech 2020*, pp. 3610–3614, 2020.
- [55] J. Yu, W. Han, A. Gulati, C.-C. Chiu, B. Li, T. N. Sainath, Y. Wu, and R. Pang, "Dual-mode asr: Unify and improve streaming asr with full-context modeling," in *ICLR*, 2021.
- [56] G. Liu, K. Gong, X. Liang, and Z. Chen, "Cp-gan: Context pyramid generative adversarial network for speech enhancement," in *ICASSP 2020-2020 IEEE International Conference on Acoustics, Speech and Signal Processing (ICASSP)*. IEEE, 2020, pp. 6624–6628.
- [57] M.-H. Hoang, S.-H. Kim, H.-J. Yang, and G.-S. Lee, "Context-aware emotion recognition based on visual relationship detection," *IEEE Access*, vol. 9, pp. 90 465–90 474, 2021.
- [58] T. Dai, J. Cai, Y. Zhang, S.-T. Xia, and L. Zhang, "Second-order attention network for single image super-resolution," in *Proceedings of the IEEE/CVF conference on computer vision and pattern recognition*, 2019, pp. 11 065–11 074.
- [59] Q. Wang, B. Wu, P. Zhu, P. Li, W. Zuo, and Q. Hu, "Eca-net: Efficient channel attention for deep convolutional neural networks," in *Proceedings of the IEEE/CVF Conference on Computer Vision and Pattern Recognition (CVPR)*, June 2020.
- [60] X. Zhang, X. Wu, X. Zhai, X. Ben, and C. Tu, "Davd-net: Deep audio-aided video decompression of talking heads," in *Proceedings of the IEEE/CVF Conference on Computer Vision and Pattern Recognition*, 2020, pp. 12 335–12 344.
- [61] A. Ghosh and R. Chellappa, "Deep feature extraction in the dct domain," in *2016 23rd International Conference on Pattern Recognition (ICPR)*. IEEE, 2016, pp. 3536–3541.
- [62] M. Ulicny and R. Dahyot, "On using cnn with dct based image data," in *Proceedings of the 19th Irish Machine Vision and Image Processing conference IMVIP*, vol. 2, 2017, pp. 1–8.
- [63] Z. Qin, P. Zhang, F. Wu, and X. Li, "Fcanet: Frequency channel attention networks," in *Proceedings of the IEEE/CVF International Conference on Computer Vision*, 2021, pp. 783–792.
- [64] M. Ehrlich and L. S. Davis, "Deep residual learning in the jpeg transform domain," in *Proceedings of the IEEE/CVF International Conference on Computer Vision*, 2019, pp. 3484–3493.
- [65] W. Xia and J. H. Hansen, "Speaker recognition with nonlinear distortion: Clipping analysis and impact," in *INTERSPEECH*, 2018, pp. 746–750.
- [66] M.-T. Luong, H. Pham, and C. D. Manning, "Effective approaches to attention-based neural machine translation," in *Proceedings of the 2015 Conference on Empirical Methods in Natural Language Processing*, 2015, pp. 1412–1421.
- [67] H. S. Heo, B.-J. Lee, J. Huh, and J. S. Chung, "Clova baseline system for the voxcelel speaker recognition challenge 2020," *arXiv preprint arXiv:2009.14153*, 2020.
- [68] I. Loshchilov and F. Hutter, "Decoupled weight decay regularization," in *International Conference on Learning Representations*, 2019.
- [69] A. Nagrani, J. S. Chung, and A. Zisserman, "Voxceleb: A large-scale speaker identification dataset," *Proc. Interspeech 2017*, pp. 2616–2620, 2017.
- [70] J. S. Chung, A. Nagrani, and A. Zisserman, "Voxceleb2: Deep speaker recognition," *Proc. Interspeech 2018*, pp. 1086–1090, 2018.
- [71] D. Snyder, G. Chen, and D. Povey, "MUSAN: A Music, Speech, and Noise Corpus," 2015, arXiv:1510.08484v1.
- [72] T. Ko, V. Peddinti, D. Povey, M. L. Seltzer, and S. Khudanpur, "A study on data augmentation of reverberant speech for robust speech recognition," in *2017 IEEE International Conference on Acoustics, Speech and Signal Processing (ICASSP)*. IEEE, 2017, pp. 5220–5224.